Bioorganic & Medicinal Chemistry Letters 19 (2009) 4183–4190

Contents lists available at ScienceDirect

Bioorganic & Medicinal Chemistry Letters

journal homepage: www.elsevier.com/locate/bmcl

Discovery and functional evaluation of diverse novel human CB_1 receptor ligands

Nicolas Foloppe [a,*], Karen Benwell [a], Teresa D. Brooks [a], Guy Kennett [b], Antony R. Knight [b], Anil Misra [b], Nathaniel J. T. Monck [b]

[a] Vernalis (R&D) Ltd, Granta Park, Abington, Cambridge, CB21 6GB, UK
[b] Vernalis (R&D) Ltd, Oakdene Court, 613 Reading Road, Winnersh, RG41 5UA, UK

ARTICLE INFO

Article history:
Received 8 May 2009
Revised 25 May 2009
Accepted 27 May 2009
Available online 2 June 2009

Keywords:
Cannabinoids
Drug design
Obesity
Pharmacophore
Virtual screening

ABSTRACT

Ligand-based virtual screening with a 3D pharmacophore led to the discovery of 30 novel, diverse and drug-like ligands of the human cannabinoid receptor 1 (hCB_1). The pharmacophore was validated with a hit rate of 16%, binding selectivity versus hCB_2, and expected functional profiles. The discovered compounds provide new tools for exploring cannabinoid pharmacology.

The cannabinoid system was initially identified as mediating the effects of the major psychoactive components of *Cannabis sativa*, Δ^9-tetrahydrocannabinol. To date, this system includes at least two receptors, CB_1 and CB_2, the biology of which has been extensively reviewed.[1–3] CB_1, a GPCR coupled to inhibitory G-proteins $G_{i/o}$, is expressed in the central nervous system where it is found on presynaptic terminals, serving to modulate neurotransmitter release. It is also found in peripheral tissue. CB_2 is primarily found in cells of the immune system. Endogenous ligands (endocannabinoids) of CB_1 and CB_2 have been discovered.

The cannabinoid system has been linked to a number of pathological conditions, in particular obesity. As it pre-disposes to other diseases, particularly type 2 diabetes and coronary heart disease,[4] obesity has become a serious public health concern. Diet and exercise provide only limited long term benefits to the majority of cases,[5] which has led to the development of pharmacological treatments for obesity.[6] Current treatments, however, are only modestly efficacious and have significant side-effects.[7] Approaches to tackle obesity have included targeting the cannabinoid system.[3,8,9]

Endocannabinoids like anandamide and 2-arachidonoyl glycerol are elevated in the plasma, adipose tissue and pancreas of obese humans and animals.[10] In genetically obese rodents endocannabinoid levels are elevated in the hypothalamus, an area of the brain that modulates feeding behavior.[11] Centrally, endocannabinoids elicit feeding behavior via activation of CB_1 receptors.[7] Peripheral CB_1 activation causes lipogenesis in adipose tissue and liver, and reduces the oxidation of free fatty acids (FFA).[12] Also, stimulation of CB_1 receptors on innervations of the gut may attenuate satiety signaling.[13,14] Therefore, an elevated endocannabinoid tone is relevant for the onset and maintenance of obesity and its co-morbidities. Thus, much pharmaceutical work has aimed to discover CB_1 antagonists/inverse agonists.[15,16]

Administration of CB_1 receptor antagonists to rodents elicited prolonged weight loss, reduced lipogenesis, increased oxidation of FFA and increased glucose uptake into muscle.[7,17] Consistent with these findings, CB_1 knock-out mice have a lean phenotype and are resistant to dietary induced obesity.[12,18] Thus, human CB_1 receptor (hCB1) antagonists have been developed as potential treatment of obesity, metabolic disorder and diabetes. In Phase III clinical trials, the hCB1 antagonist rimonabant (Sanofi-Aventis, compound **1**, Fig. 1) caused progressive and prolonged weight loss and improved associated metabolic indices.[19–21]

Unfortunately, treatment with rimonabant was also associated with psychiatric adverse events, such as mood alteration with depressive disorders and anxiety, as well as nausea and

Abbreviations: CB_1, cannabinoid receptor, subtype 1; CB_2, cannabinoid receptor, subtype 2; CNS, central nervous system; FFA, free fatty acids; GPCR, G-protein coupled receptor; MMFF, Merck molecular force-field; NA, not available; NSB, non-specific binding; SAR, structure–activity relationship; SPI, single point percent inhibition; VS, virtual screening.

* Corresponding author. Tel.: +44 (0) 1223 895 338; fax: +44 (0) 1223 895 556.
E-mail address: n.foloppe@vernalis.com (N. Foloppe).

0960-894X/$ - see front matter © 2009 Elsevier Ltd. All rights reserved.
doi:10.1016/j.bmcl.2009.05.114

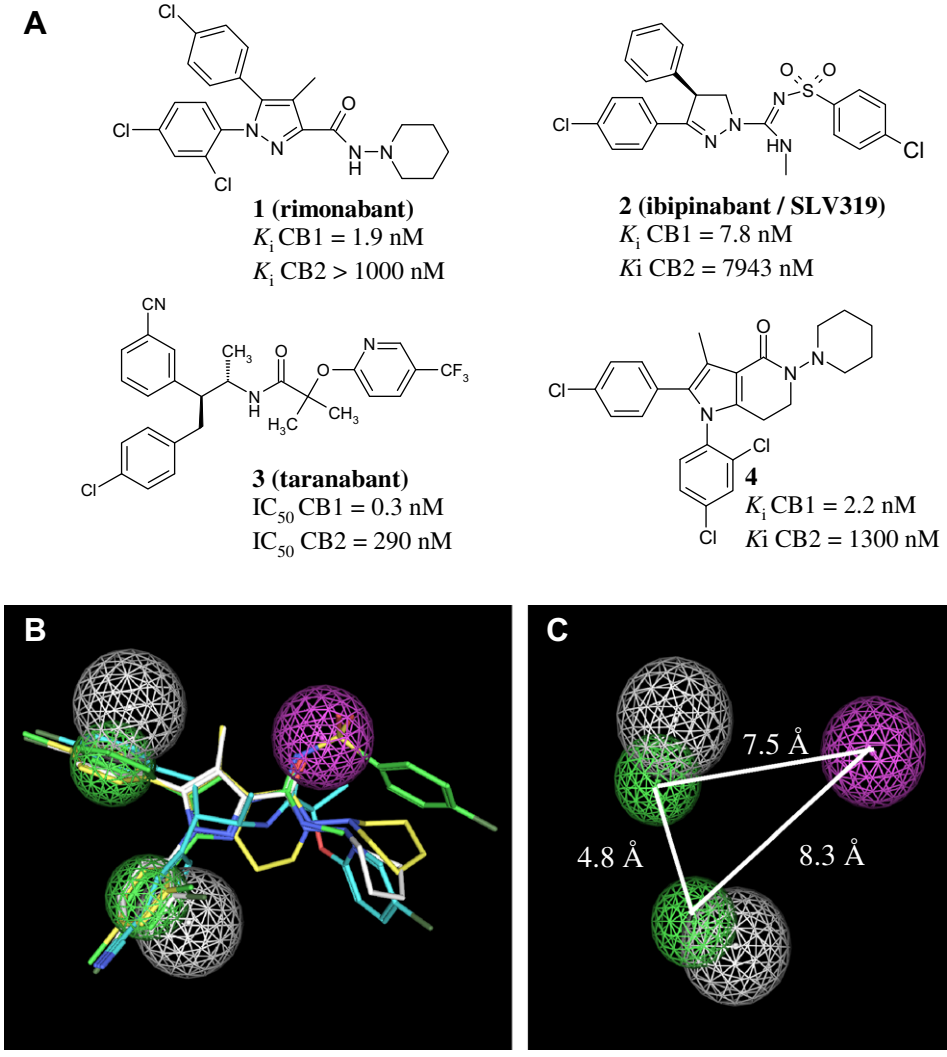

Figure 1. (A) Representative potent and selective CB_1 antagonists (**1** is rimonabant,[45] **2** is SVL319,[27] **3** is taranabant,[24] and **4** is of special interest because it constraints the position of its carbonyl hydrogen-bond acceptor.[36] The binding affinities are those reported in the cited publications. (B) A CB_1 antagonist pharmacophore derived by aligning **1** (white carbons), **2** (green carbons), **3** (cyan carbons), and **4** (yellow carbons). Nitrogens and oxygens are dark blue and red, respectively. The pharmacophore includes (i) 2 aromatic rings (green spheres; 1.5 Å tolerance radius), the projection points of the vectors normal to these rings (white spheres; 2.0 Å radius), and (ii) a hydrogen-bond acceptor (magenta sphere; 1.8 Å radius). All pharmacophoric features had to be matched to return a hit. (C) Distances (Å) between the pharmacophoric features.

dizziness.[22,23] Consequently, prescription of rimonabant was not authorized in the USA, and was recently halted in Europe. These clinical outcomes have focussed attention on the development of hCB1 antagonists with the efficacy of rimonabant, but without the psychiatric safety concerns. Alternative hCB_1 antagonists such as taranabant (**3**, Merck)[24] have been progressed to clinical studies. However taranabant was also reported to elicit depressive symptoms and anxiety in a small percentage of patients,[25,26] and its development has been terminated. The development of other hCB1 antagonists such as ibipinabant (BMS/Solvay),[27] surinabant (Sanofi-Aventis)[28] and otenabant (Pfizer)[29] were also halted.

However, the characterization of novel hCB_1 antagonists continues,[29–31] if only to improve our fundamental understanding of the CB_1 pharmacology. For instance, one possibility would be to explore the effects of targeting only the peripheral hCB_1 receptors, with compounds which would not penetrate the brain.[32] In addition, the CB_1 receptors express a range of functional responses to ligand binding, from inverse agonism to full agonism, including neutral antagonism.[33,34] The physiological and behavioural implications of these different modes of action are under intense debate,[34] which would benefit from additional pharmacological tool compounds, agonists or antagonists/inverse agonists.

Several chemical series of hCB_1 antagonists/inverse agonists have been reported and this area has been reviewed.[15,16] The vast majority of disclosed hCB_1 antagonists are close analogues or isosteres of rimonabant, including recently disclosed series derived by 'scaffold hopping'.[29,35,36] They frequently contain an aromatic cyclic core (e.g., pyrazole in **1**) substituted by two aryl moieties. For instance, these features are found in hCB_1 antagonist SLV319 (**2**),[27] and **4**[36] (of special interest for pharmacophore modeling, see below). The two distinctive aryl moieties are also present in taranabant (**3**)[24] and most disclosed hCB_1 antagonists.[15,16,31] It was proposed that the aryl groups bind to an 'aromatic microdomain' in the receptor.[37] The carbonyl hydrogen-bond acceptor of **1** was found to be important for interaction with lysine 192 in the hCB_1 receptor,[38] and this acceptor has a counterpart in other hCB_1 antagonists.[15,16,31] These features can be combined in a 3-point pharmacophore[15] for CB_1 antagonists/inverse agonists, illustrated by the alignment of **1**–**4** (Fig. 1). This alignment uses the energetically favoured conformation of rimonabant,[38] consistent with its conformationally constrained analogue **4**.[36] The pharmacophore shown in Figure 1 is similar but simpler than an alternative CB_1 antagonist pharmacophore which contained two additional hydrophobic phar-

Table 1
Structures[a] and radioligand displacement binding data[b] of the newly discovered[c] ligands of the human CB_1 receptor (hCB_1)

Structure	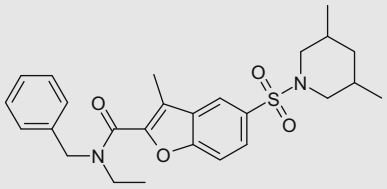	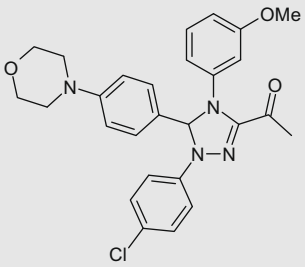	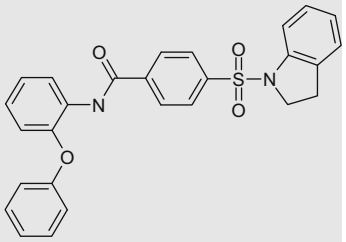
ID[d]	**5**, VER-82448	**6**, VER-82519	**7**, VER-82410
SPI (hCB_1)	98%	90%	82%
K_i hCB_1 (nM)	92	227	256
K_i hCB_2 (nM)	3100	3919	>10,000
Structure	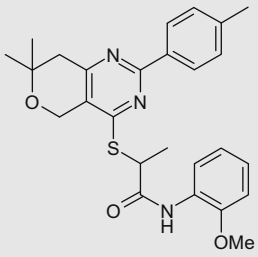	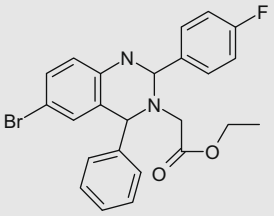	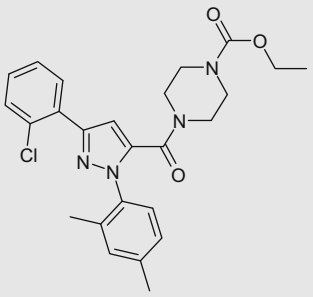
ID	**8**, VER-82497	**9**, VER-82409	**10**, VER-82319
SPI (hCB_1)	85%	77%	98%
K_i hCB_1 (nM)	264	273	287
K_i hCB_2 (nM)	>10,000	NA	1069
Structure	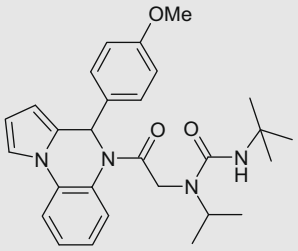	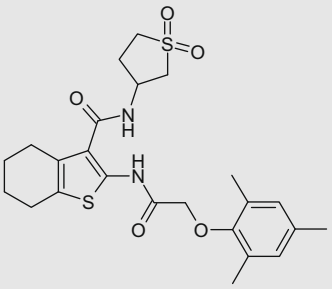	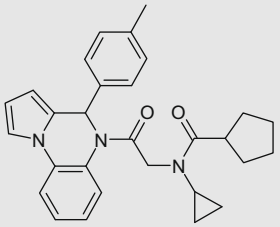
ID	**11**, VER-82317	**12**, VER-82490	**13**, VER-82315
SPI (hCB_1)	95%	94%	78%
K_i hCB_1 (nM)	308	325	520
K_i hCB_2 (nM)	4953	58	>10,000
Structure	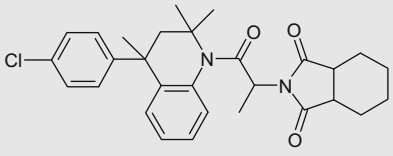	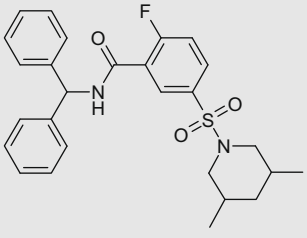	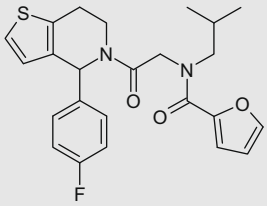
ID	**14**, VER-83053	**15**, VER-82445	**16**, VER-82311
SPI (hCB_1)	73%	77%	89%
K_i hCB_1 (nM)	520	611	875
K_i hCB_2 (nM)	NA	>10,000	NA

(*continued on next page*)

Table 1 (*continued*)

Structure	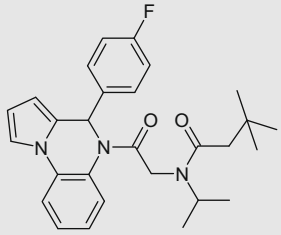	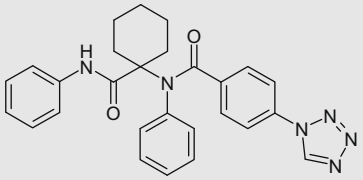	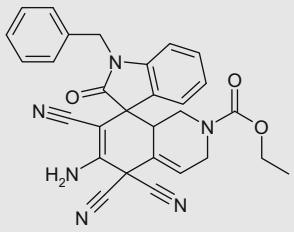
ID	**17**, VER-82316	**18**, VER-82514	**19**, VER-82524
SPI (hCB_1)	64%	71%	82%
K_i hCB_1 (nM)	1030	1049	1086
K_i hCB_2 (nM)	NA	NA	NA
Structure	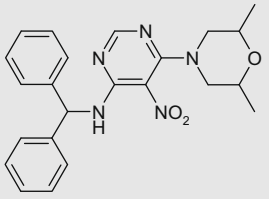	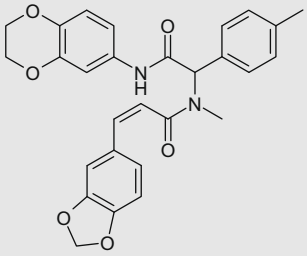	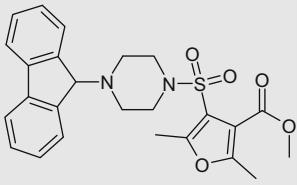
ID	**20**, VER-82827	**21**, VER-82433	**22**, VER-82330
SPI (hCB_1)	67%	71%	87%
K_i hCB_1 (nM)	1177	1473	1606
K_i hCB_2 (nM)	NA	NA	NA
Structure	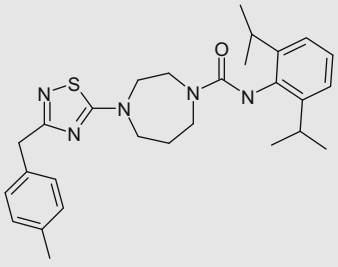	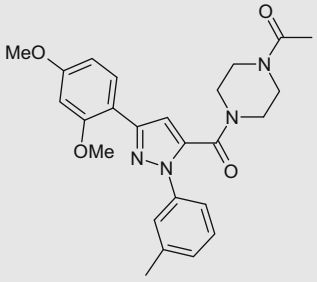	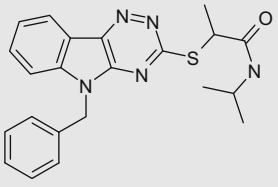
ID	**23**, VER-82313	**24**, VER-82318	**25**, VER-82303
SPI (hCB_1)	77%	77%	86%
K_i hCB_1 (nM)	1764	1943	2269
K_i hCB_2 (nM)	NA	NA	NA
Structure	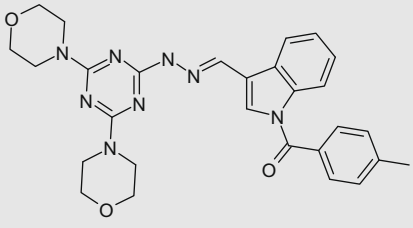	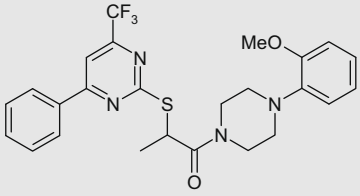	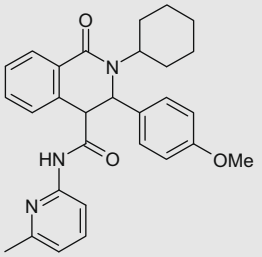
ID	**26**, VER-82411	**27**, VER-82391	**28**, VER-82430
SPI (hCB_1)	85%	80%	69%
K_i hCB_1 (nM)	2299	2314	2396
K_i hCB_2 (nM)	NA	NA	NA

Table 1 (*continued*)

Structure	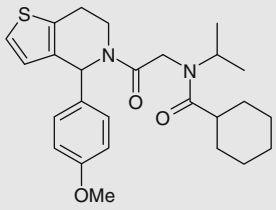	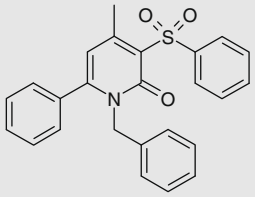	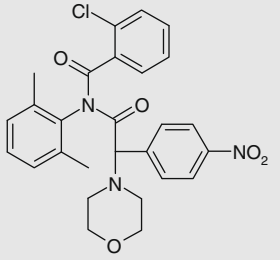
ID	**29**, VER-82312	**30**, VER-82387	**31**, VER-82399
SPI (hCB_1)	82%	73%	79%
K_i hCB_1 (nM)	2593	2716	2785
K_i hCB_2 (nM)	NA	NA	NA
Structure	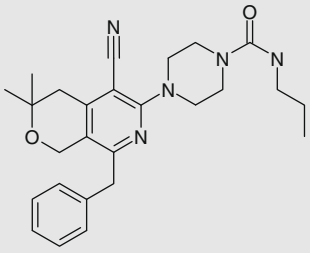	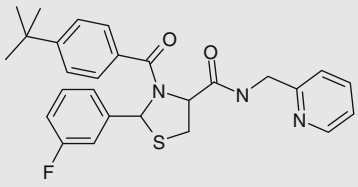	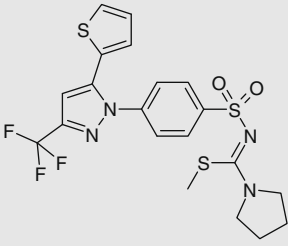
ID	**32**, VER-82423	**33**, VER-82299	**34**, VER-82328
SPI (hCB_1)	81%	62%	63%
K_i hCB_1 (nM)	3949	7490	1000
K_i hCB_2 (nM)	NA	NA	NA

NA: not available.

[a] Every compound was subjected to LC–MS analysis, and the chemical structures were consistent with the masses obtained by MS, to a purity of at least 85%. Purity was assessed by UV detection at three wavelengths and total ion current under positive ion electrospray.

[b] For initial screening, compounds were tested in duplicate at a single concentration of 10 micromolar using an experimental procedure similar to that described below for the K_i determinations. This yielded data reported as single point percent inhibition (SPI) of radioligand binding to hCB_1. Every reported K_i is the average of six measurements, obtained as detailed in Ref. 46.

[c] With the exception of previously reported[30] compound **5**.

[d] ID includes the Vernalis compound identifier.

macophoric features, and was used to discover azetidinone CB_1 ligands.[31]

The CB_1 antagonist pharmacophore shown in Figure 1 and the program Catalyst (Accelrys) were used to search the Vernalis electronic catalogue of ~700,000 commercially available compounds, pre-filtered and prepared in three-dimensional conformations as described before.[39] The query initially retrieved many hits, which were subsequently filtered on a combination of computed physico-chemical properties related to drug-likeness and compatible with CNS activity.[40–42] We discarded compounds with molecular weight >550, Slog P >6.5, number of hydrogen-bond acceptors >10, number of hydrogen-bond donors >5, and number of rotatable bonds >8 (descriptors calculated with the software MOE from Chemical Computing Group). The remaining compounds were clustered with the MACSS fingerprints[43] as implemented in MOE and a Tanimoto similarity threshold of 75%, and only one representative per cluster was kept by manual triage. This yielded 370 unique compounds which matched the pharmacophore.

Then, 261 of the 370 selected compounds were obtained from commercial vendors and assayed for binding to hCB_1 by displacement of radiolabelled rimonabant at a single compound concentration (details in Table 1). This yielded 42 compounds which exhibited greater than 60% inhibition of rimonabant binding at hCB_1, and for which quality control was satisfactory (hit rate = 16%). Of these, 30 compounds were selected for further hCB_1 K_i determination (Table 1, compounds presented by decreasing hCB_1 affinity). Their affinity for hCB_1 ranged from 92 nM (**5**) to 10 μM (**34**). Twelve compounds had submicromolar affinity for hCB_1. Compound **5** was reported previously,[30] but is included here to present a complete account of the virtual screen.

Affinity for the human CB_2 receptor (hCB_2) was also determined for 9 of the 30 hits. The selectivity ratio for these compounds, K_i (hCB_2)/K_i (hCB_1), was 33.7 (**5**), 17.3 (**6**), >39.0 (**7**), >37.9 (**8**), 3.7 (**10**), 16.1 (**11**), 0.2 (**12**), >19.2 (**13**), and >16.4 (**15**). Apart from **12**, these compounds are significantly selective for hCB_1 over hCB_2, indicating that, despite its simplicity, the pharmacophore discriminates between hCB1 and its closest known homologue receptor.

Consistent with the virtual screening selection process, the hits are chemically diverse, as confirmed by inspection of Table 1. Yet, compounds **11**, **13** and **17** represent the same scaffold; **10** and **24** also belong to a same chemical class. There is also some similarity between (i) **8** and **32** and (ii) **16** and **29**.

With their pyrazole core, **10** and **24** are reminiscent of rimonabant, however, in **10** and **24** the aryl substituents are positioned differently with respect to the core. Also, **11**, **13** and **17** are similar to a very recently disclosed series of pyrrolo[1,2-*a*]quinoxalines.[44] Thus, the scaffolds discovered by the pharmacophore search are mostly new with respect to hCB_1 binding, when assessed by comparison to other recently disclosed hCB1 ligands.[15,16,24,28,29,31,36]

Table 2
Properties[a] related to drug-likeness for the new hCB_1 ligands

ID[b]	MW[c]	Slog *P*[d]	Don[e]	Acc[f]	NRot[g]	TPSA[h]
5	468.6	5.3	0	6	7	70.8
6	491.0	5.2	0	7	6	57.6
7	470.5	5.5	1	6	6	75.7
8	463.6	5.7	1	6	6	73.3
9	469.4	5.9	2	4	5	41.6
10	467.0	4.7	0	7	6	67.7
11	474.6	5.2	1	7	7	66.8
12	490.6	3.5	2	7	6	101.6
13	453.6	5.5	0	5	7	45.5
14	493.0	5.7	0	5	4	57.7
15	480.6	5.1	1	5	6	66.5
16	440.5	4.8	0	5	8	53.8
17	461.6	5.8	0	5	7	45.5
18	480.6	5.0	1	8	7	93.0
19	504.5	3.5	1	9	4	147.2
20	419.5	4.3	1	8	6	96.1
21	486.5	4.4	1	8	7	86.3
22	466.6	3.9	1	7	4	80.1
23	491.7	6.4	1	6	7	61.4
24	448.5	3.2	0	8	7	76.9
25	405.5	4.3	1	6	6	72.7
26	526.6	2.9	1	10	7	110.0
27	502.6	5.3	0	6	7	58.6
28	469.6	5.7	1	6	5	71.5
29	454.6	5.1	0	5	8	49.8
30	415.5	5.1	0	4	5	54.5
31	508.0	5.2	1	8	8	95.7
32	447.6	3.9	1	7	6	81.5
33	477.6	5.5	1	5	6	62.3
34	500.6	5.4	0	6	5	67.6

[a] These physico-chemical properties were calculated with the software MOE.
[b] Same compound identificators as in Table 1.
[c] Molecular weight.
[d] Logarithm of the octanol/water partition coefficient.
[e] Number of hydrogen bond donors, as defined by Lipinski (lip_don descriptor in MOE).
[f] Number of hydrogen-bond acceptor, as defined by Lipinski (lip_acc descriptor in MOE).
[g] Number of rotatable bonds (b_1rotN descriptor in MOE).
[h] Topological polar surface area in $Å^2$ (TPSA descriptor in MOE).

Many of the hCB_1 ligand discovered here are arguably drug-like based on simple but widely used physico-chemical descriptors[40–42] (Table 2). There is, however, a clear trend towards lipophilic hits (e.g., 19 compounds with Slog *P* >5.0). This reflects the initial aim to discover CNS active compounds, and also the CB_1 specific pharmacophore with its two aryl groups. Less lipophilic compounds can also bind to CB1, as illustrated by 6 hits with Slog *P* <4.0. In addition, the hits are largely free from chemical functionalities with obvious medicinal chemistry liabilities, with the possible exception of **19** with its 3 nitrile groups. Of course, the compounds in Table 1 were not optimized for interaction with hCB_1 or other medicinal chemistry properties, and should be regarded as starting points for further efforts.

Elaboration of the newly discovered scaffolds may gain from considering how they fit the pharmacophore (Fig. 2). For instance, the atom which matches the pharmacophoric hydrogen-bond acceptor is not always immediately obvious from the 2D representation of the compounds. More generally, visualizing which 3D conformation/configuration of a ligand fits the pharmacophore gives indications regarding the conformational features (e.g., intramolecular hydrogen bonds) and stereochemistry (e.g. chiral centers) likely to be important to match the pharmacophore. For example, in Figure 2B the fluorophenyl of **9** is not one of the pharmacophoric aryl groups, and carbon 4 of its tetrahydropyrimidine core is in the *R* configuration to project its phenyl substituent towards a pharmacophoric point. The other compounds in Figure 2 were selected to illustrate further the chemical diversity in the output of the virtual screening.

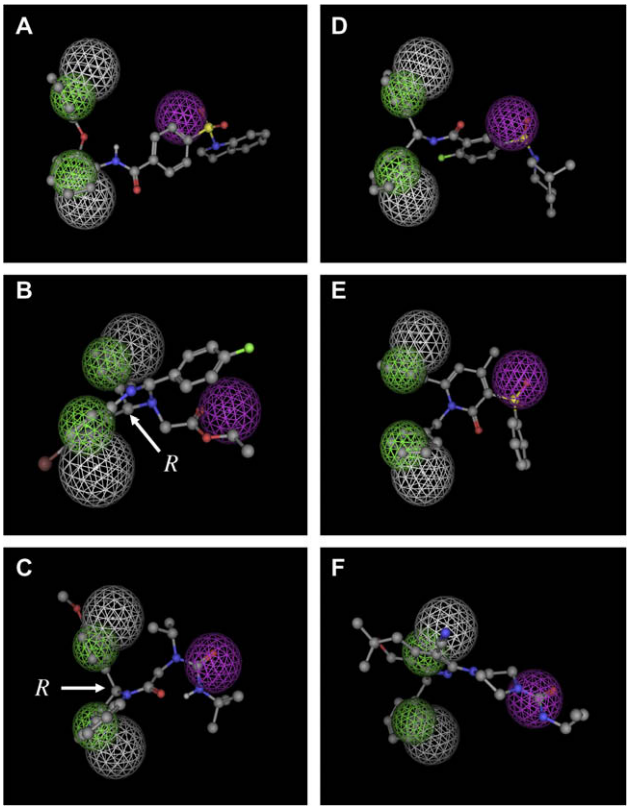

Figure 2. Depiction of how some of the discovered hCB_1 ligands reported in Table 1 match the CB_1 antagonist pharmacophore presented in Figure 1. Shown are compounds **7** (A), **9** (B), **11** (C), **15** (D), **30** (E) and **32** (F). The compounds are shown in a low energy conformation (MMFF94s force-field). The white arrows (B and C) point to chiral centers, the configuration of which (*R* or *S*, given in the panel) may be important to match the pharmacophore.

The functional response of the hCB_1 receptor was investigated for 11 of the 30 hit compounds, with a cell membrane [^{35}S]GTPγS incorporation assay (Table 3 and Fig. 3). These 11 compounds were all found to be hCB_1 inverse agonists, with EC_{50} values ranging from 0.2 to 4.4 μM (Table 3, rimonabant was used as a control). This is an additional and very strong validation of the pharmaco-

Table 3
Functional characterization[a] of some virtual screening hits

ID[b]	EC_{50} (μM)	% Efficacy relative to rimonabant
1 (rimonabant)	0.004	100
5	0.3	95
6	0.6	81
7	0.2	62
8	1.2	91
10	0.2	44
11	1.5	103
12	0.4	60
13	1.1	91
15	0.5	50
16	4.4	105
17	1.1	77

[a] The functional characterization is described in Ref. 47.
[b] Same compound identifiers as in Figure 1 and Table 1. All tested compounds were found to be inverse agonists. The EC_{50} (molar concentration which caused half the maximal response) was estimated by fitting a four-parameter logistical equation to concentration–response curves, using non-linear regression in Graphpad Prism. Each compound efficacy at eliciting a functional response is reported as a percentage of the corresponding efficacy obtained with rimonabant in the same conditions.

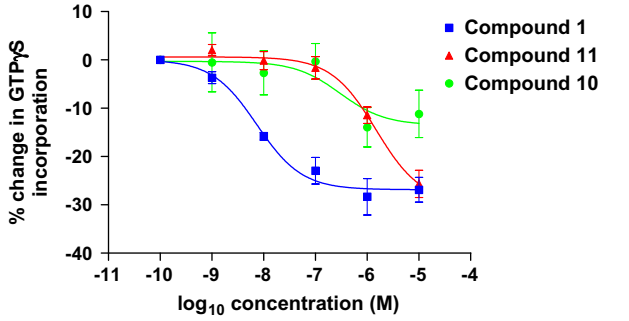

Figure 3. Effects of rimonabant (compound **1**, blue squares), compound **10** (green circles) and compound **11** (red triangles) on the binding of [^{35}S]GTPγS to G-proteins associated with hCB_1 receptors. Each point is the mean of three measurements; vertical lines show the standard error of the mean. See Table 3 for the EC_{50} values and further experimental details. Similar functional response curves were obtained for the other compounds tested in this functional assay (not shown). Compounds **1**, **10** and **11** decreased the incorporation of [^{35}S]GTPγS in a concentration-dependent manner, showing that they are inverse agonists. Compound **11** has an efficacy similar to that of rimonabant, while compound **10** is only 44% as efficacious (Table 3).

phore described in Figure 1. Interestingly, the 11 tested compounds suppress the basal level of hCB_1 activity with various efficacies relative to rimonabant, from 44% to 105% (Table 3). This diversity of functional effects on the receptor activation reflects the chemical diversity of the new hCB_1 ligands, which is of special interest for cannabinoid pharmacology. One might speculate that different inverse agonist efficacies may lead to different physiological responses in vivo, possibly with side-effect profiles that would differ from those observed clinically so far (see above).

In conclusions, we have presented a highly successful ligand-based virtual screening for the discovery of hCB_1 ligands, which validates the pharmacophore used. The diversity of the discovered scaffolds contrasts with the similarity between rimonabant and the majority of the hCB_1 antagonists disclosed so far. This, combined with the range of observed inverse agonist efficacies, offers the prospect to uncover new aspects of the pharmacology of the cannabinoid system.

Acknowledgment

We thank Tim Haymes for his support with analytical chemistry.

References and notes

1. Wilson, R. I.; Nicoll, R. A. *Science* **2002**, *296*, 678.
2. Howlett, A. C.; Barth, F.; Bonner, T. I.; Cabral, G.; Casellas, P.; Devane, W. A.; Felder, C. C.; Herkenham, M.; Mackie, K.; Martin, B. R.; Mechoulam, R.; Pertwee, R. G. *Pharmacol. Rev.* **2002**, *54*, 161.
3. Di Marzo, V. *Drug Discovery Today* **2008**, *13*, 1026.
4. Kopelman, P. G. *Nature* **2000**, *404*, 635.
5. Crawford, D.; Jeffery, R. W.; French, S. A. *Int. J. Obes.* **2000**, *24*, 1107.
6. Cooke, D.; Bloom, S. *Nat. Rev. Drug Disc.* **2006**, *5*, 919.
7. Vickers, S. P.; Kennett, G. A. *Curr. Drug Targets* **2005**, *6*, 215.
8. Pagotto, U.; Vicennati, V.; Pasquali, R. *Ann. Med.* **2005**, *37*, 270.
9. Pacher, P.; Batkai, S.; Kunos, G. *Pharmacol. Rev.* **2006**, *58*, 389.
10. Mattias, I.; Gonthier, M.-P.; Orlando, P.; Martiadis, V.; De Petrocellis, L.; Cervino, C.; Petrosino, S.; Hoareau, L.; Festy, F.; Pasquali, R.; Roche, R.; Maj, M.; Pagotto, U.; Monteleone, P.; Di Marzo, V. *J. Clin. Endocrinol. Metab.* **2006**, *91*, 3171.
11. Di Marzo, V.; Goparaju, S. K.; Wang, L.; Liu, J.; Bátkai, S.; Járai, Z.; Fezza, F.; Miura, G. I.; Palmiter, R. D.; Sugiura, T.; Kunos, G. *Nature* **2001**, *410*, 822.
12. Osei-Hyiaman, D.; Harvey-White, J.; Batkai, S.; Kunos, G. *Int. J. Obes.* **2006**, *30*, S33.
13. Gomez, R.; Navarro, M.; Ferrrer, B.; Trigo, J. M.; Bilbao, A.; Del Arco, I.; Cippitelli, A.; Nava, F.; Piomelli, D.; Rodriquez de Fonseca, F. R. *J. Neurosci.* **2002**, *22*, 9612.
14. Cani, P. D.; Montoya, M. L.; Neyrinck, A. M.; Delzenne, N. M.; Lambert, D. M. *Br. J. Nutr.* **2004**, *92*, 757.
15. Lange, J. H. M.; Kruse, C. G. *Drug Discovery Today* **2005**, *10*, 693.
16. Smith, R. A.; Fathi, Z. *IDrugs* **2005**, *8*, 53.
17. Liu, Y. L.; Connoley, I. P.; Wilson, C. A.; Stock, M. J. *Int. J. Obes.* **2005**, *29*, 183.
18. Ravinet Trillou, C.; Delgorge, C.; Menet, C.; Arnone, M.; Soubrié, P. *Int. J. Obes.* **2004**, *28*, 640.
19. Van Gaal, L. F.; Rissanen, A. M.; Scheen, A. J.; Ziegler, O.; Rössner, S. *Lancet* **2005**, *365*, 1389.
20. Despres, J.-P.; Golay, A.; Sjostrum, L. N. *Eng. J. Med.* **2005**, *353*, 2121.
21. Pi-Sunyer, F. X.; Aronne, L. J.; Heshmati, H. M.; Devin, J.; Rosenstock, J. *J. Am. Med. Assoc.* **2006**, *295*, 761.
22. Van Gaal, L.; Pi-Sunyer, X.; Despres, J.-P.; McCarthy, C.; Scheen, A. *Diabetes Care* **2008**, *31*, S229.
23. Christensen, R.; Kristensen, P. K.; Bartels, E. M.; Bliddal, H.; Astrup, A. *Lancet* **2007**, *370*, 1706.
24. Lin, L. S.; Lanza, T. J., Jr.; Jewell, J. P.; Liu, P.; Shah, S. K.; Qi, H.; Tong, X.; Wang, J.; Xu, S. S.; Fong, T. M.; Shen, C.-P.; Lao, J.; Xiao, J. C.; Shearman, L. P.; Stribling, D. S.; Rosko, K.; Strack, A.; Marsh, D. J.; Feng, Y.; Kumar, S.; Samuel, K.; Yin, W.; Van der Ploeg, L. H. T.; Goulet, M. T.; Hagmann, W. K. *J. Med. Chem.* **2006**, *49*, 7584.
25. Addy, C.; Wright, H.; Van Laere, K.; Gantz, I.; Erondu, N.; Musser, B. J.; Lu, K.; Yuan, J.; Sanabria-Bohorquez, S. M.; Stoch, A.; Stevens, C.; Fong, T. M.; De Lepeleire, I.; Cilissen, C.; Cote, J.; Rosko, K.; Gendrano, I. N.; Nguyen, A. M.; Gumbiner, B.; Rothenberg, P.; de Hoon, J.; Bormans, G.; Depre, M.; Eng, W.; Ravussin, E.; Klein, S.; Blundell, J.; Herman, G. A.; Burns, H. D.; Hargreaves, R. J.; Wagner, J.; Gottesdiener, K.; Amatruda, J. M.; Heymsfield, S. B. *Cell Metab.* **2008**, *7*, 68.
26. Addy, C.; Li, S.; Agrawal, N.; Stone, J.; Majumdar, A.; Zhong, L.; Li, H.; Yuan, J.; Maes, A.; Rothenberg, P.; Cote, J.; Rosko, K.; Cummings, C.; Warrington, S.; Boyce, M.; Gottesdiener, K.; Stoh, A.; Wagner, J. *J. Clin. Pharmacol.* **2008**, *48*, 738.
27. Lange, J. H. M.; Coolen, H. K. A. C.; van Stuivenberg, H. H.; Dijksman, J. A. R.; Herremans, A. H. J.; Ronken, E.; Keizer, H. G.; Tipker, K.; McCreary, A. C.; Veerman, W.; Wals, H. C.; Stork, B.; Verveer, P. C.; den Hartog, A. P.; de Jong, N. M. J.; Adolfs, T. J. P.; Hoogendoorn, J.; Kruse, C. G. *J. Med. Chem.* **2004**, *47*, 627.
28. Rinaldi-Carmona, M.; Barth, F.; Congy, C.; Martinez, S.; Oustric, D.; Perio, A.; Poncelet, M.; Maruani, J.; Arnone, M.; Finance, O.; Soubrie, P.; Le Fur, G. *J. Pharmacol. Exp. Ther.* **2004**, *310*, 905.
29. Griffith, D. A.; Hadcock, J. R.; Black, S. C.; Iredale, P. A.; Carpino, P. A.; DaSilva-Jardine, P.; Day, R.; Dibrino, J.; Dow, R. L.; Landis, M. S.; O'Connor, R. E.; Scott, D. O. *J. Med. Chem.* **2009**, *52*, 234.
30. Foloppe, N.; Allen, N. H.; Bentley, C. H.; Brooks, T. D.; Kennett, G.; Knight, A. R.; Leonardi, S.; Misra, A.; Monck, N. J. T.; Sellwood, D. M. *Bioorg. Med. Chem. Lett.* **2008**, *18*, 1199.
31. Wang, H.; Duffy, R. A.; Boykow, G. C.; Chackalamannil, S.; Madison, V. S. *J. Med. Chem.* **2008**, *51*, 2439.
32. Kunos, G.; Osei-Hyiaman, D.; Batkai, S.; Sharkey, K. A.; Makriyannis, A. *TIPS* **2008**, *30*, 1.
33. Pertwee, R. G. *Life Sci.* **2005**, *76*, 1307.
34. Salamone, J. D.; McLaughlin, P. J.; Sink, K.; Makriyinnis, A.; Parker, L. A. *Physiol. Behav* **2007**, *91*, 383.
35. Bostrom, J.; Berggren, K.; Elebring, T.; Greasley, P. J.; Wilstermann, M. *Bioorg. Med. Chem.* **2007**, *15*, 4077.
36. Smith, R. A.; Fathi, Z.; Brown, S.-E.; Choi, S.; Fan, J.; Jenkins, S.; Kluender, H. C. E.; Konkar, A.; Lavoie, R.; Mays, R.; Natoli, J.; O'Connor, S. J.; Ortiz, A. A.; Podlogar, B.; Taing, C.; Tomlinson, S.; Tritto, T.; Zhang, Z. *Bioorg. Med. Chem. Lett.* **2007**, *17*, 673.
37. McAllister, S. D.; Rizvi, G.; Anavi-Goffer, S.; Hurst, D. P.; Barnett-Norris, J.; Lynch, D. L.; Reggio, P. H.; Abood, M. E. *J. Med. Chem.* **2003**, *46*, 5139.
38. Hurst, D. P.; Lynch, D. L.; Barnett-Norris, J.; Hyatt, S. M.; Seltzman, H. H.; Zhong, M.; Song, Z.-H.; Nie, J.; Lewis, D.; Reggio, P. *Mol. Pharmacol.* **2002**, *62*, 1274.
39. Foloppe, N.; Fisher, L. M.; Howes, R.; Potter, A.; Robertson, A. G. S.; Surgenor, A. E. *Bioorg. Med. Chem.* **2006**, *14*, 4792.
40. Lipinski, C. A.; Lombardo, F.; Dominy, B. W.; Feeney, P. J. *Adv. Drug Delivery Rev.* **1997**, *23*, 3.
41. Kelder, J.; Grootenhuis, P. D. J.; Bayada, D. M.; Delbressine, L. P. C.; Ploemen, J.-P. *Pharm. Res.* **1999**, *16*, 1514.
42. Veber, D. F.; Johnson, S. R.; Cheng, H.-Y.; Smith, B. R.; Ward, K. W.; Kopple, K. D. *J. Med. Chem.* **2002**, *45*, 2615.
43. McGregor, M. J.; Pallai, P. V. *J. Chem. Inf. Comput. Sci.* **1997**, *37*, 443.
44. Szabó, G.; Kiss, R.; Páyer-Lengyel, D.; Vukics, K.; Szikra, J.; Baki, A.; Molnár, L.; Fischer, J.; Keserua, G. M. *Bioorg. Med. Chem. Lett.*, in press.
45. Rinaldi-Carmona, M.; Barth, F.; Héaulme, M.; Shire, D.; Calandra, B.; Congy, C.; Martinez, S.; Maruani, J.; Néliat, G.; Caput, D.; Ferrara, P.; Soubrié, P.; Brelière, J. C.; Le Fur, G. *FEBS Lett.* **1994**, *350*, 240.
46. Protocol for the measurement of the K_i data presented in Table 1. The affinity of compounds for the hCB_1 receptor was determined based on a published method. [36]HEK293 cells transfected to express the human CB_1 receptor were grown using standard tissue culture procedures. Cell pellets were homogenised in 80 volumes (v/v) of 50 mM Tris–HCl buffer (pH 7.4) containing 5 mM $MgCl_2$, 2.5 mM EDTA and 0.5 mg/ml BSA using an Ultra-Turrax homogeniser. For the assay, cell membranes were incubated in a total volume of 250 μl, containing tritiated rimonabant (1 nM final concentration, Amersham TRK1028), and test compounds at a range of concentrations. Non-specific binding was determined using CP 55,940 (10 μM). Following a 90 min incubation at 30 °C, assays were terminated by rapid filtration with GF/B filters (pre-soaked in 0.1% (w/v) polyethylenimine) using a Canberra Packard filtermate 196. Microscint-20 scintillation fluid was added to the filters, which were soaked for at least 2 h before counting on a liquid scintillation

spectrophotometer (Packard TopCount). IC_{50} values were estimated using a logistical equation in XLfit (IDBS); K_i values were calculated from these using the Cheng–Prusoff conversion.

47. The functional characterization in Table 3 was obtained by monitoring G-protein activation via the exchange of GDP for the non-hydrolysable GTP analogue [^{35}S]GTPγS, using a cell membrane incorporation assay. Human CB_1 membranes (4 μg per well, Perkin Elmer) were incubated for 60 min at 37 °C, in assay buffer containing 20 mM Hepes, 100 mM NaCl, 32 mM $MgCl_2$, 1 μM GDP, 0.1 nM [^{35}S]GTPγS and varying concentrations of tested hCB_1 ligand in 0.1% DMSO (final volume 250 μl per well in a 96-well plate). Non-specific binding (NSB) was determined using an excess of GTP (10 μM) in the absence of tested compound. The reaction was terminated by rapid filtration under vacuum, through GF/B filterplates (pre-soaked in distilled water). The plates were washed four times with 250 μl of ice-cold assay buffer and the bound radioactivity counted on a Topcount scintillation counter. Activity of the compounds was determined as the percentage change from basal binding (in the absence of cannabinoid ligand, after subtraction of NSB). Data was a mean of 3 replicates.